Comparative Biochemistry and Physiology, Part C 248 (2021) 109101

Contents lists available at ScienceDirect

Comparative Biochemistry and Physiology, Part C

journal homepage: www.elsevier.com/locate/cbpc

Transporter-interfering chemicals inhibit P-glycoprotein of yellowfin tuna (*Thunnus albacares*)

Sascha C.T. Nicklisch [a], Amara K. Pouv [a], Steven D. Rees [b], Aaron P. McGrath [b], Geoffrey Chang [b], Amro Hamdoun [c,*]

[a] Department of Environmental Toxicology, University of California, Davis, Davis, CA 95616, United States of America
[b] Skaggs School of Pharmacy and Pharmaceutical Sciences, 9500 Gilman Drive #0754, University of California, San Diego, La Jolla, CA 92093, United States of America
[c] Center for Marine Biotechnology and Biomedicine, Scripps Institution of Oceanography, University of California, San Diego, La Jolla, CA 92093-0202, United States of America

ARTICLE INFO

Edited by Martin Grosell

Keywords:
Yellowfin tuna
P-glycoprotein
ABC transporter
Persistent organic pollutants
Bioaccumulation
Transporter-interfering chemicals
DDT
ABCB1
marine pollution
fish physiology

ABSTRACT

Marine pollutants bioaccumulate at high trophic levels of marine food webs and are transferred to humans through consumption of apex species. Yellowfin tuna (*Thunnus albacares*) are marine predators, and one of largest commercial fisheries in the world. Previous studies have shown that yellowfin tuna can accumulate high levels of persistent organic pollutants, including Transporter Interfering Chemicals (TICs), which are chemicals shown to bind to mammalian xenobiotic transporters and interfere with their function. Here, we examined the extent to which these same compounds might interfere with the activity of the yellowfin tuna (*Thunnus albacares*) ortholog of this transporter. To accomplish this goal we identified, expressed, and functionally assayed tuna ABCB1. The results demonstrated a common mode of vertebrate ABCB1 interaction with TICs that predicts effects across these species, based on high conservation of specific interacting residues. Importantly several TICs showed potent inhibition of *Ta*-ABCB1, such as the organochlorine pesticides Endrin ($EC_{50} = 1.2 \pm 0.2$ μM) and Mirex ($EC_{50} = 2.3 \pm 0.9$ μM). However, unlike the effects observed on mouse ABCB1, low concentrations of the organochlorine pesticide TICs p,p'-DDT and its metabolite p,p'-DDD co-stimulated verapamil-induced *Ta*-ABCB1 ATPase activity possibly suggesting a low transport activity for these ligands in tuna. These results provide a mechanistic basis for understanding the potential vulnerability of tuna to these ubquitous pollutants.

1. Introduction

Yellowfin tuna are apex marine predators that inhabit tropical and subtropical waters around the world. This species accounts for the world's second largest tuna fishery with annual landings in excess of 1.25 million pounds (Pecoraro et al., 2018, 2017). As apex predators they can accumulate high levels of marine pollutants, with the primary concern about these pollutants on their potential transfer to humans who eat the tuna (Choy et al., 2009; Nicklisch et al., 2017a, 2017b; Pulster et al., 2020; Xie et al., 2020). Less understood are the potential impacts of these bioaccumulative pollutants on the tuna themselves. Fish share many of the pathways targeted by pollutants in mammals and thus are likely to have many similar effects form pollutant exposure. For example, both embryonic fish and mammals share cardiac ion channels sensitive to polyaromatic hydrocarbons found in air pollution and crude oil spills (Brette et al., 2014; Holme et al., 2019; Incardona et al., 2014, 2013, 2009, 2005, 2004; Marris et al., 2020). As such the pollutants carried in fish not only represent a hazard to the humans who consume them, but also to the fish themselves.

One of the cellular pathways on which many organic contaminants converge are xenobiotic transporters (XTs). These conserved proteins evolved to protect against toxic foreign molecules in diet and the

Abbreviations: MDR, multidrug resistance; ABC transporter, ATP-binding cassette transporter; TIC, Transporter-interfering chemical; XT, xenobiotic transporter; RACE, rapid amplification of cDNA ends; CAM, Calcein-AM; Ta, *Thunnus albacares*.

* Corresponding author at: Center for Marine Biotechnology and Biomedicine, Scripps Institution of Oceanography, UC San Diego, 9500 Gilman Drive #0202, Hubbs Hall 3150, La Jolla, CA 92093-0202, United States of America.
E-mail addresses: nicklisch@ucdavis.edu (S.C.T. Nicklisch), akpouv@ucdavis.edu (A.K. Pouv), sdrees@ucsd.edu (S.D. Rees), g1chang@ucsd.edu (G. Chang), hamdoun@ucsd.edu (A. Hamdoun).

https://doi.org/10.1016/j.cbpc.2021.109101
Received 4 April 2021; Received in revised form 7 May 2021; Accepted 31 May 2021
Available online 8 June 2021

environment. Among XTs, several ATP-binding cassette (ABC) transporters including ABCB1 (P-glycoprotein), ABCC1, and ABCG2, are ubiquitously expressed in biological barriers, including kidney, liver, brain and intestine, and act to limit the cellular entry and accumulation of diverse xenobiotics by binding and effluxing them (Dean et al., 2001; Giacomini et al., 2010; Nicklisch and Hamdoun, 2020). P-glycoprotein or ABCB1 is a major determinant of human drug disposition. As such it, and its orthologs, are structurally and functionally one of the best characterized xenobiotic efflux pumps (Ambudkar et al., 2003; Bosch and Croop, 1998; Callaghan, 2015; Morrissey et al., 2012; Palmeira et al., 2012) with currently over 350 known drug substrates (https://go.drugbank.com).

Persistent environmental chemicals which bioaccumulate in apex marine predators also bind to these transporters, but rather than being effectively eliminated, they can inhibit their function (Nicklisch et al., 2016; Sreeramulu et al., 2007; Xie et al., 2020). Of concern is that the interfering action of these chemicals on xenobiotic metabolism can limit the normal detoxification capacity of XTs. Transporter-Interfering Chemicals (TICs) are environmentally ubiquitous compounds, including persistent organic pollutants (POPs), such as organochlorine pesticides, brominated flame retardants (brominated diphenyl ethers or BDEs) and polychlorinated biphenyls. We previously showed nine of these that were commonly detected in tuna (Nicklisch et al., 2017a). These included the brominated flame retardants BDE-47 and BDE-100, both of which showed high levels of accumulation between 1 and 3 ppb in yellowfin tuna in comparison to other BDE congener flame retardants (Nicklisch et al., 2017a).

The goal of this study was to understand the similarities and differences in TIC effects between tuna and murine ABCB1 – one of the major xenobiotic transporters in vertebrates. In our previous study (Nicklisch et al., 2016), we demonstrated that persistent environmental chemicals can intimately interact with the ligand binding domain of this protein. The co-crystal structure of mouse ABCB1a in complex with one of these two flame retardants, BDE-100, showed an intricate network of hydrophobic and electrostatic interactions of the pollutant deep within a ligand binding site of the transporter. Importantly, 87% of the residues across the full protein sequence and those interacting with the bound flame-retardant are conserved between mouse and human homologs, suggesting potential conservation of this site. However, given the promiscuity of ABCB1 for its ligands it remains uncertain whether TIC interactions can be extrapolated across species as divergent as fish and mice.

To accomplish this goal, we cloned and expressed functional *Ta*-ABCB1 and probed the purified, protein against the same TIC compounds found in tuna, and shown to inhibit mouse and human ABCB1. The results demonstrated a common mode of vertebrate ABCB1 interaction with TICs that predicts effects across these species, based on high conservation of specific interacting residues, with two important implications. The first is that ubiquitous TICs such as persistent pollutants could act at multiple steps in the food chain in a sort of positive feedback loop to amplify inhibitory effects that lead to enhanced pollutant bioaccumulation. The second is that TICs could act to sensitize yellowfin tuna themselves to exposures in their environment. This could be of particular relevance for populations with high TIC exposure.

2. Materials and methods

2.1. Chemicals

Cyclosporine A (CSA), verapamil (VER), Triton X-100, and dimethyl sulfoxide (DMSO) were purchased from Sigma (St. Louis, MO, USA). Calcein-AM (CAM) was purchased from Biotium (Hayward, CA). Except for verapamil (dissolved in H_2O), all stock solutions were prepared in DMSO and diluted to final concentrations in filtered seawater. The final DMSO concentration in the ATPase and cell assays did not exceed 2% and 0.5%, respectively.

2.2. Animal and tissue handling

Mature yellowfin tuna (*Thunnus albacares*) organs were extracted from wild tuna caught off the coast of Louisiana in the Gulf of Mexico. The fish had an average length of 111–185 cm (Nicklisch et al., 2017a). Samples were shock-frozen in dry ice and stored at −80 °C until total RNA extraction or homogenization. Purple sea urchins (*Strongylocentrotus purpuratus*) were collected and maintained in aquaria as detailed previously (Campanale and Hamdoun, 2012).

2.3. Tuna tissue homogenization and immunoblotting

Approximately 100 mg tuna tissue was dissected on dry ice. Tools were disinfected with 70% ethanol in between tissue preparations. A 1:9 (w/v) ratio of tuna tissue and 3× homogenization buffer (RIPA buffer, EDTA-free protease inhibitor tablets (Pierce EDTA-free) was transferred to 2 mL centrifuge tubes with 2.8 mm ceramic beads (Omni International) and twice homogenized in a bead mill (Fisherbrand Bead Mill 24) Samples were incubated on ice for 30 min prior to transferring the homogenate into 1.5 mL centrifuge tubes and centrifuging at 15,000 x g for 2 min at 4 °C. The supernatant was stored at −80 °C until use. *Ta*-ABCB1 detection was performed using the C219 anti-P-glycoprotein antibody (van Den Elsen et al., 1999). The SDS mini-gels were hand-cast using standard reagents to create a 4% stacking and 7.5% resolving gel. Approximately 20 μg of total lysate protein was separated on a 7.5% SDS gel (Laemmli, 1970). Gels were transferred to a 0.2 um PVDF membrane for 30 min at 100 V using a mini-PROTEAN II system (Biorad). Membranes were blocked for 1 h in 5% BSA in TBST (20 mM Tris and 150 mM NaCl with 0.1% Tween 20, pH 7.6). Primary mouse C219 monoclonal anti-P-glycoprotein (Invitrogen) was added in a 1:1000 dilution and incubated overnight (16 h at 4 °C). Membrane was washed 3 times for 10 min each in TBST then incubated for 1 h at RT in secondary goat anti-mouse (BioRad) diluted at 1:10,000 in 5% BSA in TBST. Membrane was washed 3 times in TBST for 10 min each and then developed using Clarity Western ECL (BioRad). Images were taken in a BioRad ChemiDoc station using the ImageLab software v6.0.1.

2.4. Cloning and subcloning of Ta-abcb1

Primers were designed based on highly conserved regions among fish ABCB1 orthologs. The oligonucleotides were obtained from IDT (Coralville, Iowa, USA). Total RNA was isolated from approximately 30 mg of liver tissue of wild yellowfin tuna from the Gulf of Mexico using an RNA II kit (Macherey-Nagel, Düren, Germany) and reverse transcribed using the RNA-to-cDNA kit according to the manufacturer's instructions (High-Capacity RNA-to-cDNA Kit, Applied Biosystems, Foster City, CA, USA). PCR was performed in a GeneAmp PCR System 9700 thermal cycler (Applied Biosystems, Foster City, CA, USA) using Phusion high fidelity DNA polymerase (New England Biolabs, Ipswich, MA, USA). 5′- and 3′ ends of the gene were cloned from RACE-ready cDNA using the SMARTer RACE cDNA Amplification Kit (Clontech, Mountain View, CA, USA). The full-length sequence of the transporter (3894 bps) was cloned into the *Pichia* expression plasmid pPICZc (Invitrogen, Carlsbad, CA, USA) harboring a C-terminal 3C Protease site and C-terminal His_6-tag or into the pCS2 + 8 vector harboring an N-terminal mCherry tag (Gökirmak et al., 2012). The *Ta-abcb1* cDNA generated in this study is available through the Addgene (www.addgene.org) public repository.

2.5. Ta-abcb1 overexpression and purification

Ta-ABCB1 was expressed and purified as described previously (Nicklisch et al., 2016). Briefly, the gene was cloned into a pPICZc vector and mutagenized to remove potential N-glycosylation sites (N101Q, N104Q, N109Q, and N116Q, using codon CAA in these positions). The deglycosylated construct was transformed into *P. pastoris* strain KM71H (ThermoFisher Scientific, Waltham, MA, USA) using a GenePulser Xcell

electroporation system (BioRad). Resulting clones were grown in 10-L BioFlo 415 bioreactors (New Brunswick Scientific, Edison, NJ, USA) and induced for 16–18 h with a 2.5% flow rate of 50% MeOH. A typical 10-L growth would typically yield 20–40 mg of protein. Resulting cells were harvested by centrifugation and lysed at 40 KPSI by a single pass through a cell disruptor (TS-Series, Constant Systems, Daventry, Northants, UK). Cell debris was removed by centrifugation at 12,500 ×g, followed by membrane isolation at 38,400 ×g into lysis buffer (20 mM Tris pH 8.0, 100 mM NaCl, 15% glycerol). Membranes were solubilized and *Ta-ABCB1* was purified using a Ni–nitrilotriacetic acid Superflow resin (Qiagen) via fast protein liquid chromatography (AEKTA, GE Life Sciences). The protein was concentrated at 1500 ×g (Millipore, Burlington, MA, USA), and a single, monomeric peak was isolated by size exclusion chromatography using a prep-grade Superdex 200 column (Fisher Scientific). The calculated molecular mass of *Ta*-ABCB1 (1297aa) is ~143.3 kDa (http://web.expasy.org/protparam/). The total concentration of the purified protein was determined using the Micro BCA Protein Assay Kit (Pierce, Rockford, lL, USA). Protein purity was evaluated by combined 7.5% SDS PAGE and wet electroblotting on 0.45 mM PVDF using a primary mouse 6-His Epitope Tag monoclonal antibody (1:2000) and secondary goat anti-mouse IgG-HRP (1:5000) in 5% skim milk/TBST (0.1 M Tris-base, 150 mM NaCl, 0.05% Tween 20). The proteins were visualized using the SuperSignal West Pico Chemiluminescent Substrate kit (Pierce, Rockford, lL, USA).

2.6. MALDI mass spectrometry analysis

The molecular mass of the purified, recombinant *Ta*-ABCB1 was determined using Matrix-assisted laser desorption ionization (MALDI) mass spectrometry analysis with time-of-flight (TOF) detector. The analysis was performed on a Voyager Mass Spectrometer LBT2 (Applied Biosystems, San Jose, CA) with 1.2-m ion path in the positive ion linear mode. As matrix solution, sinapinic acid in 50% acetonitrile and 0.1% trifluoroacetic acid (TFA) was used. Samples were diluted 1:20 with matrix solution and 1 µL was spotted onto the MALDI sample target plates and air-dried on the bench. Spectra were obtained in the mass range between 5000 and 200,000 Da with 256 laser shots per spectrum. Internal calibration was performed using bovine serum albumin standard (Sigma-Aldrich, St. Louis, MO) with a calculated molecular mass of 66.5 kDa. All data was analyzed using Voyager Data Explorer 4.0.0.0 (Applied Biosystems) and plotted using OriginPro 2016 (Originlab, Northampton, MA).

2.7. ATPase activity of solubilized Ta-ABCB1

For the determination of *Ta*-ABCB1 ATPase activity we used a modified malachite green assay for detection of inorganic phosphate (Pi) release as described previously (Nicklisch et al., 2016). Briefly, 2 µg of purified and solubilized *Ta*-ABCB1 activated protein was added to a 96 well plate containing 60 µL of ATP-free reaction buffer (10 mM $MgSO_4$, 0.05% w/v DDM, 1 mM TCEP, 0.1 mg/mL *E. coli* Polar Extract lipids in 50 mM Tris-Cl buffer pH 7.5) with serial dilutions of verapamil or cyclosporin A with 100 µM verapamil. Then 60 µL of ATP solution (5 mM Na-ATP, 10 mM $MgSO_4$, 0.05% w/v DDM, 1 mM TCEP, 0.1 mg/mL *E. coli* Polar Extract lipids in 50 mM Tris-Cl buffer pH 7.5) was added, mixed and incubated for 5 min on ice. After incubation, the reaction mixtures in the 96 well PCR plate were transferred to a thermocycler and the reaction was kept for 5 min at 37 °C before a 15 s incubation at 80 °C (heat inactivation). 30 µL of the ATPase reactions were transferred to a 96 well ELISA plate and the liberated Pi was measured by adding 150 µL of an activated stock color development solution (17 mg malachite green in 3.75 mL MilliQ H_2O, 0.525 g ammonium molybdate tetrahydrate in 12.5 mL of 4 N HCl, activated with 0.02% v/v Triton X-100) in each sample well. The absorbance of each sample was immediately measured at 600 nm in a microplate reader (Spectramax M2, Sunnyvale, CA, US). Control samples containing buffer and DMSO (cyclosporine A) or H_2O (verapamil) without any added ABCB1 protein were subtracted as background values. Inorganic phosphate standards (KH_2PO_4) from 0.125 to 2 nmol served as internal controls.

2.8. Ta-ABCB1 efflux activity assays in sea urchin embryos

Efflux activity was determined at ~16 h post fertilization (hpf) in embryos expressing *Ta*-ABCB1 protein with N-terminal fluorescent mCherry tag as previously described (Gökirmak et al., 2014). Embryos were incubated with CAM at a final concentration of 250 nM at 15 °C for 90 min. Intracellular accumulation was measured using a Zeiss (Jena, Deutschland) LSM 700 laser scanning confocal microscope equipped with a 20× objective. 4.1 µm thick equatorial section images of 10–28 embryos from two separate experiments (2 different females) were collected for the transporter-drug pair.

2.9. Phylogenetic analysis

Using the software CLC Main Workbench v21.0.2 (Qiagen N.V., Hilden, Germany), multi-sequence alignments and phylogenetic trees were created. Briefly, protein sequences for ABCB1 orthologs of vertebrate model organisms were first identified using the Kyoto Encyclopedia of Genes and Genomes (KEGG) reference pathway on ABC transporters. The reference protein sequences were then downloaded from the National Center for Biotechnology Information (NCBI) *Reference Sequence Database* (RefSeq). Additional orthologous vertebrate genes and proteins were identified using *NCBI Orthologs* search based on NCBI's Eukaryotic Genome Annotation pipeline. Truncated proteins and additional protein isoforms (IF) or variants (e.g., X1, X2, etc.) with identical amino acid sequences were omitted from the phylogenetic analysis. All protein sequence alignments were performed using the integrated algorithm for progressive alignments with a gap open cost of 10 and a gap extension cost of 1. Gaps at the ends of each sequence were treated like gaps in any other place in the sequence. Distance-based tree construction was performed with neighbor joining method and Jukes-Cantor protein distance measure and based on 1000 bootstrap iterations. Alternative tree construction methods using the unweighted pair group method with arithmetic mean (UPGMA) and the Kimura protein distance measure algorithm resulted in similar tree topologies and confirmed that distance measures were robust. Amino acid sequences in an alignment were additionally analyzed for percent sequence identity and differences using the *Pairwise Comparison* algorithm of CLC Main Workbench. Each comparison table displays the differences in alignment position in the upper comparison and the percentage of identical amino acid alignment positions in the lower comparison.

2.10. Transport kinetic data analysis

ATPase activity data are given as means ±standard error of the mean (SEM) from triplicate measurements. To calculate EC_{50} values, the data were fitted to a Hill function: $y = v_1 + (v_2 - v_1) * x^n / (k^n + x^n)$, where v_1 and v_2 are the initial and final reaction velocities, respectively, n is the Hill coefficient or the cooperativity of the dependence on x, and k is the effective concentration (EC_{50}) that corresponds to 50% of maximal effect (i.e., inhibition or stimulation). All studies were performed in 3–5 independent experiments and representative experiments are shown. All calculations were performed using OriginPro 2016 software (Originlab, Northampton, MA). For the sea urchin embryo dye efflux experiments, the average efflux activity of each transporter was calculated by measuring the intracellular substrate fluorescence intensity per pixel in microinjected embryos relative to control embryos using measurement module of the free image processing software Fiji (i.e., ImageJ).

3. Results

3.1. Cloning of Ta-abcb1 from tuna liver

A full-length *Ta-abcb1* gene (*Ta*-ABCB1) was cloned from liver samples with a full-length ORF of 3894 bp, resulting in a full-length protein of 1297 amino acids (Fig. S1). To identify possible isoforms of the gene, we screened 3–4 sets of additional liver sample cDNAs with gene-specific end-to-end primers (Table S1). An alignment of the *Ta-abcb1* gene sequences cloned from these four liver samples only showed three synonymous SNPs that did not alter the amino acid sequence of the *Ta*-ABCB1 protein. Structural motifs unique to the catalytic ABC domain were identified in both nucleotide binding domains (NBDs) of *Ta*-ABCB1 (Fig. S1). Using TOPCONS (https://topcons.net/pred/) consensus prediction server, a topology analysis of *Ta*-ABCB1 amino acid sequence was performed and revealed 12 distinct transmembrane domains with cytoplasmic N- and C-termini, characteristic for other ABCB1 homologs (Fig. S2). A protein-protein BLAST (BLASTP) analysis of the full-length *Ta*-ABCB1 amino acid sequence showed high sequence similarity with other fish ABCB1 orthologues (Table S2).

3.2. Phylogenetic analysis of Ta-ABCB1

The phylogenetic analysis based on amino acid sequence alignments revealed that *Ta*-ABCB1 clusters with ABCB1/B4 orthologs of fish and other vertebrate species (Fig. 1). This subcluster is distinct from the group of ABCB5 orthologues and the evolutionarily distant *S. purpuratus* ABCB1a protein. The topology of the tree suggests that the annotated *X. tropicalis* ABCB1 transporter (XP_017951387) has a closer evolutionary relationship to the ABCB5 orthologues. Amino acid sequence comparison between *Ta*-ABCB1 and vertebrate ABCB1 orthologs (Fig. 1, inserts) shows 74% sequence identity to ABCB4 of model fish species *D. rerio* and only 53% sequence identity to *D. rerio* ABCB5, the two identified P-glycoproteins in zebrafish (Fischer et al., 2013; Gordon et al., 2019; Robey et al., 2021). Interestingly Southern Platyfish (*X. maculatus*) ABCB1/4 had 80.1% sequence identity to *Ta*-ABCB1.

Tuna ABCB1 showed slightly higher sequence identity to human ABCB1 (62.4%) versus rat ABCB1a (62.2%) or mouse ABCB1a (62.0%). Indeed, in rat a total of 491 alignment positions differed from tuna ABCB1, while mouse ABCB1a differed by 496 positions (Fig. 1, lower insert). The comparison of all non-fish vertebrate species revealed that chicken ABCB1 has the highest sequence identity to tuna ABCB1 with 64% and only 469 amino acid positions differing (Fig. 1, lower insert). Despite being an evolutionarily distant deuterostome, the sequence

	Ta-ABCB1	Sp-MDR1	Xm-MDR1	Ga-P-gp	Fh-ABCB1	Pf-MDR1	Nf-MDR1	Ol-MDR1	Om-ABCB1 X1	Tr-MDR1 X1	Dr-ABCB4	Aa-ABCB4
	1	2	3	4	5	6	7	8	9	10	11	12
Ta-ABCB1 1		254	259	261	262	263	272	274	276	294	337	387
Sp-MDR1 2	80.43		247	247	256	250	264	262	323	300	370	395
Xm-MDR1 3	80.05	80.96		48	120	66	194	224	320	305	365	392
Ga-P-gp 4	79.89	80.96	96.29		118	70	193	222	308	307	368	388
Fh-ABCB1 5	79.82	80.26	90.74	90.90		124	193	217	308	304	358	378
Pf-MDR1 6	79.75	80.74	94.91	94.60	90.43		195	225	311	305	370	394
Nf-MDR1 7	79.04	79.65	85.01	85.09	85.10	84.95		239	329	308	390	386
Ol-MDR1 8	78.91	79.82	82.72	82.87	83.23	82.64	81.54		331	315	372	387
Om-ABCB1 X1 9	78.72	75.06	75.35	76.27	76.18	76.06	74.63	74.46		346	300	341
Tr-MDR1 X1 10	77.38	76.87	76.52	76.37	76.60	76.54	76.25	75.71	73.28		374	401
Dr-ABCB4 11	74.04	71.45	71.90	71.67	72.33	71.54	69.98	71.34	76.67	71.12		332
Aa-ABCB4 12	70.44	69.78	70.03	70.34	70.99	69.92	70.38	70.37	73.73	69.20	74.40	

	Ta-ABCB1	Gga-ABCB1	Xt-ABCB1 lf2	Hs-ABCB1	Rn-ABCB1a	Mm-ABCB1a	Oc-ABCB1	Xl-ABCB1	Mm-ABCB1b	Rn-ABCB1b	Spu-ABCB1a
	1	2	3	4	5	6	7	8	9	10	11
Ta-ABCB1 1		469	489	491	493	496	502	512	519	520	730
Gga-ABCB1 2	64.06		429	391	405	403	405	445	430	432	704
Xt-ABCB1 lf2 3	62.50	67.03		423	412	416	434	139	462	460	699
Hs-ABCB1 4	62.38	69.78	67.54		167	163	167	439	250	247	712
Rn-ABCB1a 5	62.22	68.60	68.26	86.95		66	201	432	208	195	694
Mm-ABCB1a 6	61.99	68.81	68.00	87.27	94.83		206	432	208	220	696
Oc-ABCB1 7	61.53	68.70	66.69	86.96	84.30	83.91		454	280	281	717
Xl-ABCB1 8	60.83	65.87	89.22	66.39	66.79	66.85	65.24		475	472	707
Mm-ABCB1b 9	60.23	66.74	64.54	80.50	83.74	83.76	78.16	63.63		84	708
Rn-ABCB1b 10	60.15	66.59	64.70	80.73	84.75	82.83	78.06	63.86	93.42		706
Spu-ABCB1a 11	46.17	47.93	48.30	47.45	48.59	48.52	47.08	47.82	47.79	47.94	

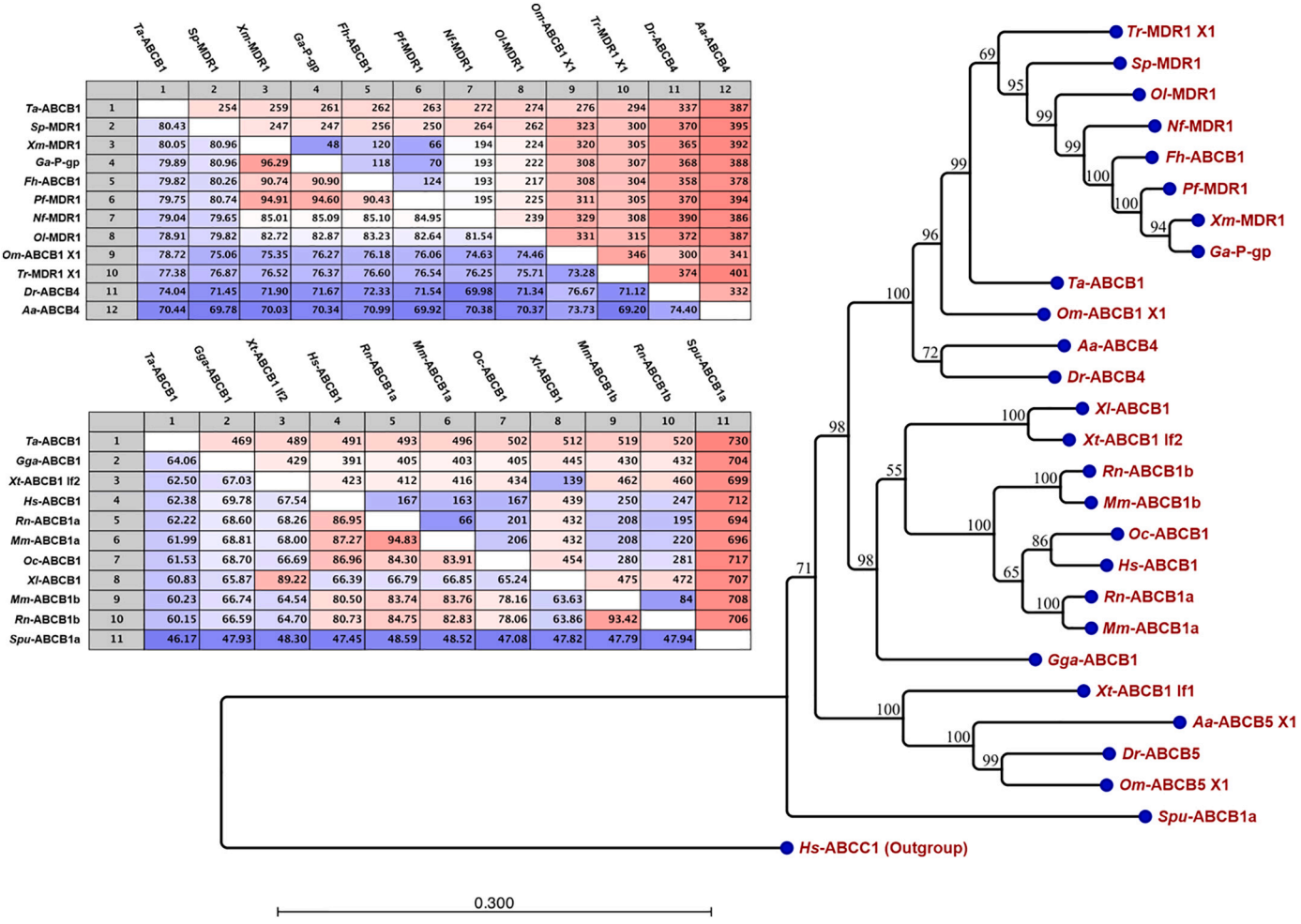

Fig. 1. Phylogenetic analysis and sequence comparison of full length *T.a.*-ABCB1 with ABCB1 homologs of vertebrates. The percentage concordance based on 1000 bootstrap iterations is shown at the nodes. Table inserts: Pairwise comparison of amino acid sequences and their percent identities (lower comparison) and differences (upper comparison) separated by fish (upper panel) and other vertebrate (lower panel) ABCB1 homologs. Ta, *Thunnus albacares; sp, stegastes partitus*; Xm, *Xiphophorus maculatus*; Ga, *Gambusia affinis*; Fh, *Fundulus heteroclitus*; Pf, *Poecilotheria formosa*; Nf, *Nothobranchius furzeri*; Ol, *Oryzias latipes*; Om, *Oncorhynchus mykiss*; Tr, *Takifugu rubripes*; Dr., *Danio rerio*; Aa, *Anguilla anguilla*; Gga, *Gallus gallus*; Xt, *Xenopus tropicalis*; Hs, *Homo sapiens*; Rn, *Rattus norvegicus*; Mm, *Mus musculus*; Oc, *Oryctolagus cuniculus*; Xl, *Xenopus laevis*; Spu, *Strongylocentrotus purpuratus*.

identity between *Ta*-ABCB1 and sea urchin ABCB1a is still 46.2%. The pairwise comparison of fish model organisms ABCB1 orthologs showed high amino acid sequence identities to tuna ABCB1, ranging from 70.4% in the catadromous European eel (*A. anguilla*) to 80.4% in bicolor Damselfish (*S. partitus*), a tropical reef fish (Fig. 1, upper insert).

Although we refer to the identified tuna gene as *abcb1*, we note the fact that several teleost fish possess at least two ABCB/P-glycoprotein-like co-orthologues with xenobiotic efflux function, commonly referred to as *abcb4* and *abcb5* (Fischer et al., 2013; Gordon et al., 2019; Liu et al., 2013; Luckenbach et al., 2014). While these proteins share many functions with mammalian ABCB1, the designation of *D. rerio* ABCB4 is based on synteny analysis, rather than a similar function in export of bile acids to mammalian ABCB4. As such final nomenclature for our identified tuna ABCB transporter must await successful chromosomal analysis of *Ta*-ABCB1.

3.3. *Ta-ABCB1 expression and purification*

A challenge of cellular assays of transporter activity against pollutants is the confounding effect of background transporters (Nicklisch and Hamdoun, 2020). To address this issue and better characterize the activity of *Ta*-ABCB1 against pollutants we expressed the protein at mg scale in yeast (*Pichia pastoris*) and purified it using combined affinity tag and size exclusion chromatography. While a mixture of βDDM, CHS, and CHAPS were used during purification of *Ta*-ABCB1, use of βDDM alone was sufficient for subsequent functional assays. Native *Ta*-ABCB1 with a molecular mass of approximately 170–200 kDa was detected in liver, gill, brain, and gonads using the C219 anti-P-glycoprotein monoclonal antibody (Fig. 2A). The predicted molecular mass of recombinant *Ta*-ABCB1 with the four mutated N-glycosylation sites, a protease cleavage site, and affinity tag is 146 kDa which could be confirmed using MALDI TOF mass spectrometry (Fig. 2B). The 7.5% SDS-gel and Anti-His_6-tag Western blot in Fig. 2B (insert) show that no major contaminants or degradation products were detected during the purification process.

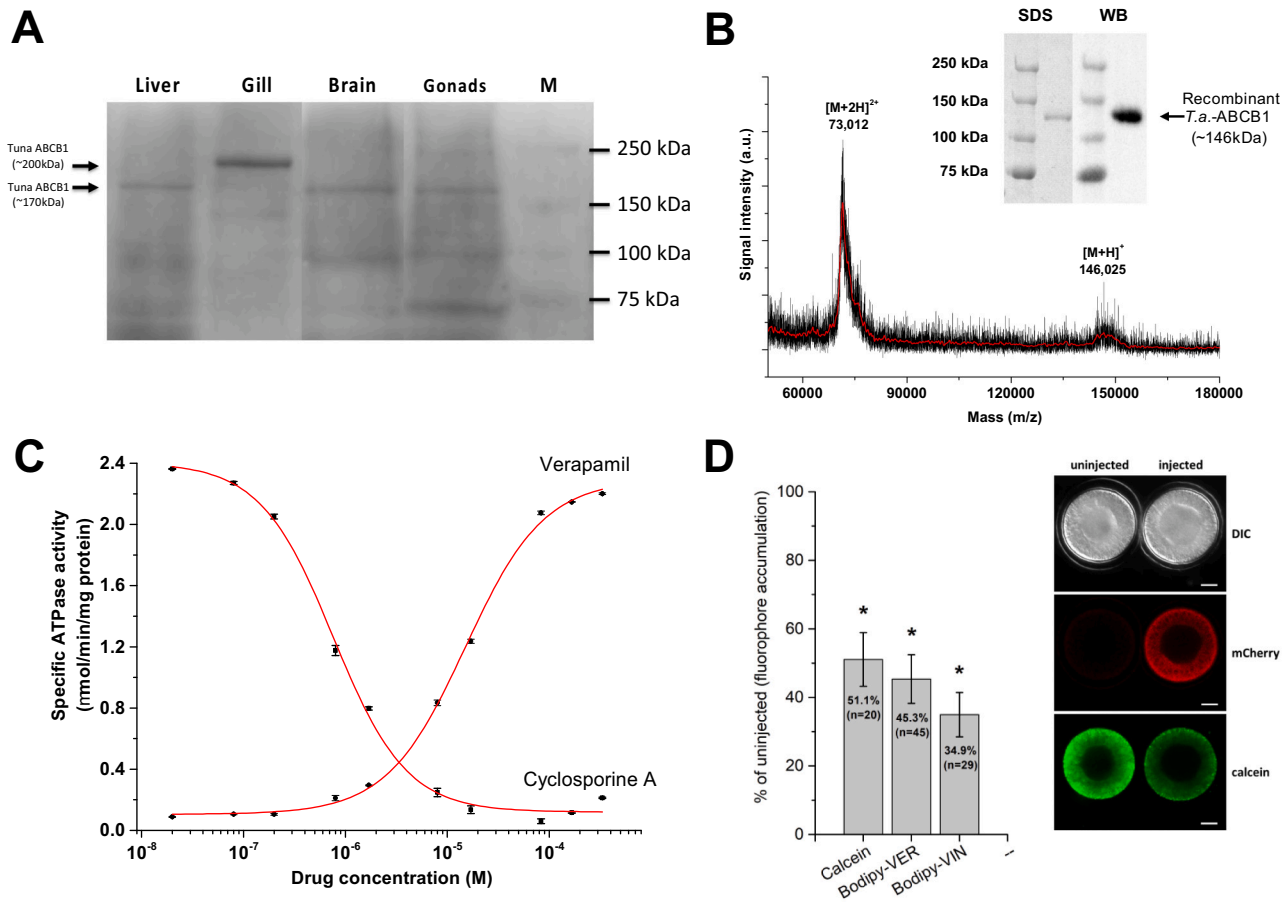

Fig. 2. Detection, purification, and activity of tuna ABCB1 (*T.a.*-ABCB1). A: PVDF Immunoblot of yellowfin tuna tissue extracts using C219 mAB, Extracts were separated with a 7.5% SDS PAGE gel. Liver, gonad, and brain extracts show a sharp protein band at ~170 kDa with minor degradation bands, and gills have a band at ~200 kDa indicating protein glycosylation. B: MALDI TOF mass spectrum of the purified *Ta*-ABCB1 with two differently charged species. The addition of a C-terminal 3C protease site (LEVLFQGP) and His10–tag (HHHHHHHHHH) leads to an observed mass of about 146 kDa. Noise reduction of the data was done by adjacent averaging (weighted average) with a window of $n = 100$ points (red trace). Matrix = Sinapinic acid, Accelerating voltage = 25,000 V, Grid voltage = 93%, Guide wire voltage = 0.3, Delay time = 700 ms. Insert: 7.5% SDS-PAGE with Coomassie blue staining (left) and an immunoblot of *Ta*-ABCB1 fused to a C-terminal His_{10}-tag by anti-His antibody (right) of purified *Ta*-ABCB1. C: ATPase activity of purified *Ta*-ABCB1 using the malachite green method. ATPase activation and inhibition were determined with increasing concentrations of verapamil and cyclosporine A. Data points indicate the average specific activity ±SEM from three to six independent experiments. Where not visible, error bars are smaller than the symbols. Lines represent non-linear regression analysis of the data points with a Hill equation ($y = v_1 + (v_2 - v_1) * x_n / (k_n + x_n)$). R^2 values for the data fits were between >0.99. D: Quantitative analysis of intracellular fluorophore accumulation in purple sea urchin (*S. purpuratus*) embryos expressing *Ta*-ABCB1. Asterisk indicates that the difference between the means of uninjected and injected embryos was significant at the level of $\alpha = 0.05$ (one-way ANOVA). Representative apical localization of N-terminal mCherry-tagged *Ta*-ABCB1 transporter in 16 hpf embryos (right panel). The DIC image shows blastulae with a single cell layer of polarized cells. Scale bars: 20 μm. $n = 37$ embryos from 3 separate batches. (For interpretation of the references to color in this figure legend, the reader is referred to the web version of this article.)

3.4. ATPase activity of detergent-solubilized Ta-ABCB1

To examine whether the *Ta*-ABCB1 gene we cloned encodes a functional transporter, we used an optimized ATPase assay based on the sensitive malachite green method requiring only 1 μg of total protein per well (Nicklisch et al., 2016). Fig. 2C shows the respective dose–response curves for the model substrates verapamil and the model inhibitor cyclosporine A with tuna ABCB1. Activating *Ta*-ABCB1 ATPase activity using verapamil resulted in a half-maximal stimulation concentration (EC_{50} value) of 8.8 ± 0.6 μM, like what was found for mouse ABCB1a (Bai et al., 2011; Swartz et al., 2013). Verapamil-stimulated (100 μM) *Ta*-ABCB1 was inhibited in the presence of increasing concentrations of cyclosporine A with an EC_{50} value of 1.3 ± 0.1 μM. Cyclosporine A restored *Ta*-ABCB1 back to the basal activity level (~0.1 μmol/min/mg protein).

3.5. Dye efflux assays of Ta-ABCB1 expressed in sea urchin embryos

To validate transporter localization and efflux activity in a marine cell, we used a well- established transporter overexpression method in purple sea urchin embryos (Gokirmak et al., 2016; Gökirmak et al., 2014, 2012; Shipp et al., 2015). In this assay the mRNA encoding the transporter fused to a fluorescent protein reporter is injected into sea urchin embryos. At 16 h after fertilization the embryo forms a polarized blastula, and the localization and efflux function of the overexpressed transporter can readily be assayed using fluorescent substrates and confocal microscopy. The results revealed that embryos overexpressing *Ta*-ABCB1 have reduced intracellular accumulation of the three fluorescent ABCB1 substrates calcein, BODIPY-verapamil, and BODIPY-vinblastine (Gökirmak et al., 2014; Litman et al., 2000). Fig. 2D shows the quantitative and qualitative analysis of intracellular accumulation in sea urchin embryos expressing tuna ABCB1 fused to an N-terminal mCherry tag. *Ta*-ABCB1 fused to an N- or C-terminal mCherry tag localized apically at 16 HPF (hours post fertilization) and led to reduction of intracellular accumulation of calcein. *Ta*-ABCB1 overexpressing embryos accumulated 51.1%, 45.3%, and 34.9% of BODIPY-verapamil, and BODIPY-vinblastine as compared to the control embryos ($p < 0.05$, one-way ANOVA). The N-terminal mCherry fusion showed a more distinct apical localization of active *Ta*-ABCB1 as has been observed with other fluorescently tagged ABCB1 proteins (Gökirmak et al., 2012). Embryos injected with the C-terminal mCherry fusion did not produce mature tuna ABC transporter as gauged by fluorescence.

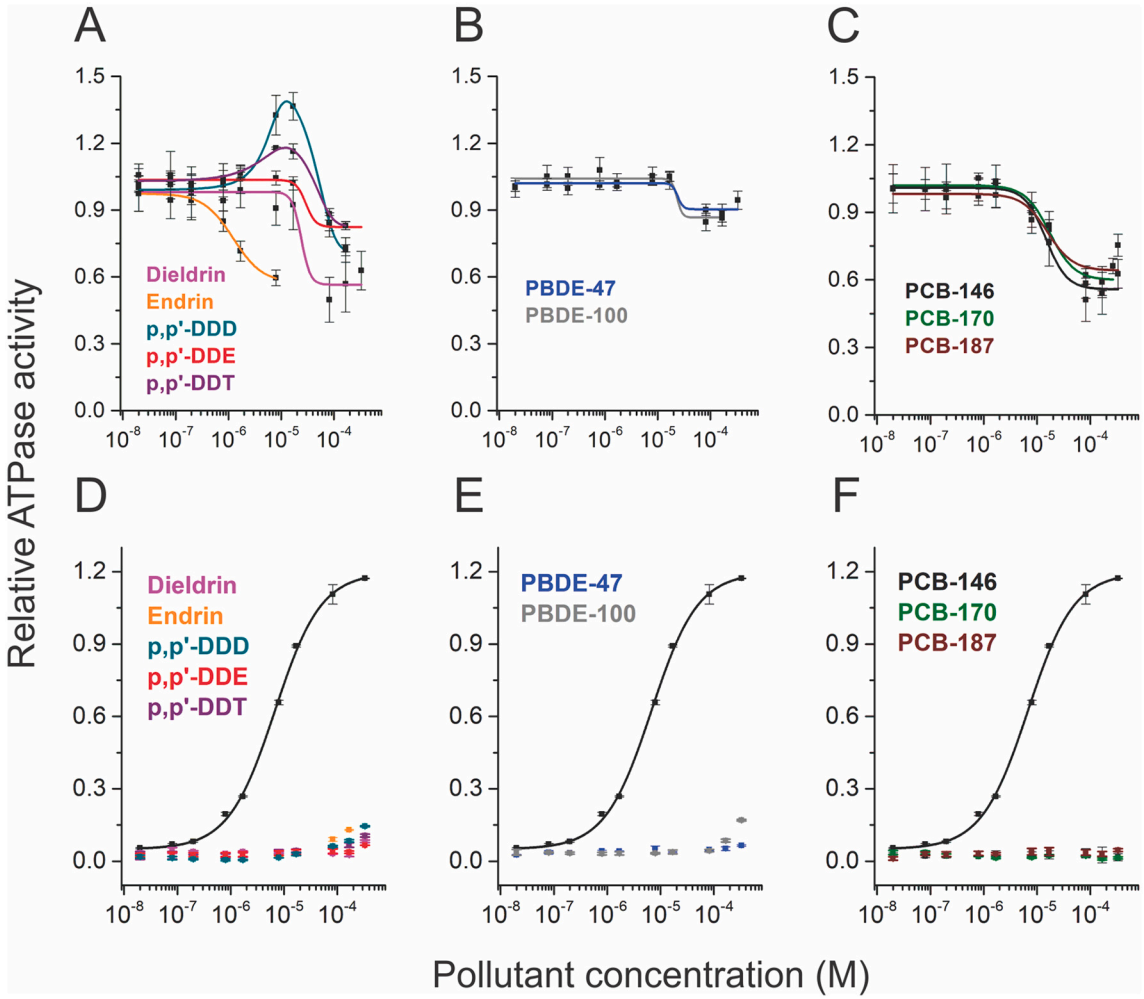

Fig. 3. ATPase activity assays of *Ta*-ABCB1 with Transporter-Interfering Chemicals (TICs). Upper panels show the inhibition profiles of the five organochlorine pesticides (A), two flame retardants (B) and three polychlorinated biphenyl (PCB) congeners (C) that were previously identified to inhibit mouse ABCB1a. Lower panels show *Ta*-ABCB1 ATPase activity assays in stimulation mode. The five pesticides (D), two flame retardants (E), and three PCBs (F) were not able to stimulate ATPase activity. Black curves show verapamil stimulation. All data points were normalized to 100 μM verapamil stimulation and indicate the average relative ATPase activity ±SEM from at least three to six independent experiments. Where not visible, error bars are smaller than the symbols. Lines represent non-linear regression analysis of the data points with a Hill equation ($y = v_1 + (v_2 - v_1) * x_n / (k_n + x_n)$). R^2 values for data fits were > 0.99.

3.6. Molecular interactions of Ta-ABCB1 with environmental chemicals

3.6.1. Conserved inhibition kinetics with transporter-interfering chemicals (TICs)

Next, we examined the interaction of known TICs with tuna ABCB1 (Fig. 3). The ATPase assay can be conducted in activation mode to identify possible transporter substrates and in inhibition mode to identify both compounds that block transporter activity or do only weakly interact (Nicklisch and Hamdoun, 2020). Consistent to what was found with mouse ABCB1a (Nicklisch et al., 2016), all TICs inhibited verapamil-stimulated *Ta*-ABCB1 ATPase activity (Fig. 3A–C). In activation mode, TICs were unable to stimulate *Ta*-ABCB1 ATPase activity as compared to model stimulator verapamil (Fig. 3D–F). The observed stereoselectivity for mouse ABCB1a inhibition by the two TICs Endrin and Dieldrin was also conserved in *Ta*-ABCB1, with Endrin having an EC_{50} value of 1.2 ± 0.2 μM and Dieldrin of 26.4 ± 6.5 μM (Table 1, Fig. 3A). Like what was observed for human ABCB1 (IC_{50} = 27.7 μM) and mouse ABCB1a (IC_{50} = 25.2 μM) (Nicklisch et al., 2016), an environmental mixture of TICs showed additive inhibitory effects on *Ta*-ABCB1 with an EC_{50} of 24.7 μM (Table 1).

3.6.2. Differences in Ta-ABCB1 interaction kinetics with DDT and BDE compounds among TICs

The inhibition curves for p,p'-DDD and p,p'-DDT showed an unexpected pattern: At low concentrations (<0.17 μM), there was no change in verapamil-stimulated ATPase activity. However, at test concentrations of 0.33, 1.67 and 3.33 μM, a pronounced stimulation of ATPase activity was observed, that declined with further increase in pollutant concentrations at 16.67, 33.33 and 166.7 μM (Fig. 3A). While both pollutants showed no stimulation in the absence of verapamil at these concentrations (Fig. 3D), the results indicate a type of co-stimulation of verapamil and DDD or DDT at relatively low pollutant concentrations (Litman et al., 1997; Orlowski et al., 1996; Shapiro and Ling, 1997; Shapiro et al., 1999). The EC_{50} values of the brominated flame retardant BDE-100 (21.9 ± 5.7 μM) was comparable to what was observed for mouse ABCB1a (Fig. 3B, Table 1). However, half-maximal inhibitory concentration of BDE-47 towards *Ta*-ABCB1 was about twice as high as with mouse ABCB1a (Fig. 3B, Table 1).

3.6.3. Non-TIC interactions show potent inhibition in mouse and tuna

We further examined the interaction profiles of 19 additional persistent organic pollutants (POPs) and an environmental TIC mixture with *Ta*-ABCB1 according to Nicklisch et al., 2016 (Fig. 4, Table 1). The results show that most transporter interaction kinetics were conserved (Fig. 4), including potent inhibition by the OC pesticide Mirex in tuna (EC_{50} = 2.3 ± 0.9 μM) and mouse (EC_{50} = 3.0 ± 0.2 μM), and weak interaction of both transporters with OC pesticide Hexachlorobenzene (Table 1). The fully brominated flame retardant BDE-209 showed highly similar inhibition with mouse ABCB1a (EC_{50} = 6.5 ± 0.4 μM) and tuna ABCB1 (EC_{50} = 8.9 ± 2.4 μM). However, the singly brominated BDE-3 was able to inhibit verapamil-stimulated *Ta*-ABCB1 ATPase activity (EC_{50} = 83.0 ± 2.0 μM) but showed weak interaction with the mouse transporter (Table 1).

3.7. Similarities of TIC interacting residues across other widely consumed fish species

The co-crystal structure of mouse ABCB1a with BDE-100 revealed an intricate network of transporter:environmental chemical interactions, mediated by eleven hydrophobic and four hydrophilic amino acids (Nicklisch et al., 2016; Nicklisch and Hamdoun, 2020). Ten of these fifteen interacting residues are different from known ABCB1 inhibitor interaction sites and have not been described before (Table S3), indicating that environmental chemicals inhibit ABCB1 function by a novel

Table 1
Observed kinetic parameters for the interaction of model drug stimulator, inhibitors and persistent organic pollutants (POPs) with purified *Ta*-ABCB1 protein. Marked in bold and italics are the 10 identified TICs from our previous study. MW = molecular weight in Da. Log K_{ow} = calculated octanol water partition coefficient according to PubChem (https://pubchem.ncbi.nlm.nih.gov). EC_{50} = effective concentration or concentration of a compound at which 50% of its maximum effect (i.e., inhibition or stimulation) is reached. Mouse ABCB1a EC_{50} values and TIC mixture composition according to (Nicklisch et al., 2016). NI = no/weak interaction. NA = not available. S.D. = standard deviation.

Compound	MW	Log K_{ow}	Tuna	Mouse
			EC_{50} ± S.D (μM)	EC_{50} ± S.D (μM)
Verapamil	454.6	3.8	8.8 ± 0.6	9.4 ± 0.4
Cyclosporine A	1202.6	7.5	1.3 ± 0.1	1.3 ± 0.1
Valspodar (PSC-833)	1214.6	7.7	1.4 ± 0.2	0.3 ± 0.1
Aldrin	364.9	6.5	31.2 ± 7.2	26.2 ± 1.9
Dieldrin	380.9	5.4	26.4 ± 6.5	21.8 ± 4.2
Endrin	380.9	5.1	1.2 ± 0.2	1.1 ± 0.7
Hexachlorobenzene	284.8	5.7	NI	NI
Mirex	545.6	5.3	2.3 ± 0.9	3.0 ± 0.2
p,p'-DDD	318.0	6.1	52.6 ± 2.8	72.5 ± 5.7
p,p'-DDE	318.0	6.8	27.7 ± 15.7	31.3 ± 3.7
p,p'-DDT	354.5	6.5	46.7 ± 2.1	25.6 ± 4.8
BDE-100	564.7	6.9	21.9 ± 5.7	23.2 ± 2.9
BDE-209	959.2	6.3	8.9 ± 2.4	6.5 ± 0.4
BDE-3	249.1	4.34	83.0 ± 2.0	NI
BDE-47	485.8	6.2	45.4 ± 52.7	22.6 ± 6.2
BDE-47-3-OH	501.8	NA	50.5 ± 8.1	95.7 ± 3.6
BDE-49	485.8	6.2	32.2 ± 5.2	35.6 ± 5.4
PCB-118	326.4	6.6	25.2 ± 2.5	15.9 ± 1.0
PCB-134	360.9	6.6	19.7 ± 3.9	12.5 ± 0.8
PCB-142	360.9	6.6	18.2 ± 2.2	6.1 ± 0.7
PCB-145	360.9	6.2	9.5 ± 0.9	4.4 ± 0.4
PCB-146	360.9	6.9	14.7 ± 2.3	12.8 ± 1.9
PCB-147	360.9	6.5	18.0 ± 1.7	23.6 ± 3.1
PCB-152	360.9	6.1	17.1 ± 3.8	22.1 ± 4.2
PCB-153	360.9	6.8	44.1 ± 43.6	21.8 ± 3.1
PCB-154	360.9	6.7	47.8 ± 29.0	14.3 ± 1.1
PCB-161	360.9	6.8	20.9 ± 5.6	43.2 ± 8.3
PCB-168	360.9	6.8	19.4 ± 0.3	25.8 ± 3.7
PCB-169	360.9	7.4	19.5 ± 3.3	9.7 ± 0.5
PCB-170	395.3	7.1	17.4 ± 4.2	9.2 ± 0.8
PCB-186	395.3	6.7	13.0 ± 1.4	6.9 ± 0.5
PCB-187	395.3	7.0	15.8 ± 6.9	11.6 ± 0.6
TIC mixture	NA	NA	24.7 ± 5.4	25.2 ± 1.3

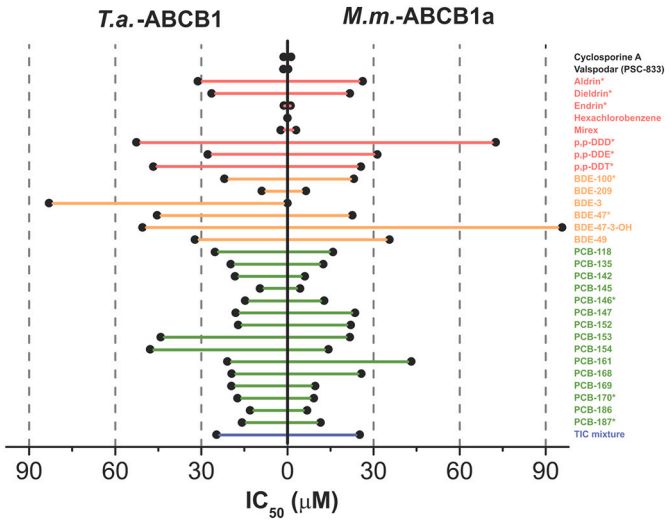

Fig. 4. Comparison of ATPase inhibition coefficients of purified mouse ABCB1a and tuna ABCB1 for model inhibitor drugs and 30 POPs. The stiff diagram displays the determined IC_{50} vales for each tested pollutant compound relative to 100 μM verapamil-stimulated ATPase activity. Marked with an asterisk are the previously identified ten TICs. The TIC mixture was prepared according to previous work (Nicklisch et al., 2016). IC_{50} = inhibition coefficient or concentration of compound that inhibited 50% of maximal ATPase activity.

mode of interaction that is distinct from pharmaceutical inhibitors. Interestingly, an amino acid alignment of ABCB1 orthologs from eight common commercial fish species with tuna and human ABCB1 shows that 14 out of the 15 BDE-interacting residues are identical (Fig. 5), suggesting that the TIC effects we describe here could be widespread. Notably, the only residue that is different is in all species either a phenylalanine (F979 in mouse, F983 in human) or a tyrosine (Y), two aromatic amino acids only differing in the hydroxyl group on tyrosine. Previous studies have shown that ABCB1 often uses both tyrosine and phenylalanine residues to bind to structurally diverse ligands via a combination of hydrophobic and hydrogen bonding interactions (Chufan et al., 2016; Gutmann et al., 2010), suggesting that either of these aromatic amino acids could interact with BDE-100 and possibly other TICs. The conservation of TIC-interacting residues in human ABCB1 and its orthologs could be an opportune way to predict trophic transfer and pollutant bioaccumulation in humans and food organisms.

4. Discussion

Understanding the interactions of pharmaceutical compounds with xenobiotic transporters is part of how we predict how the human body will handle those pharmaceuticals. By the same token, understanding how xenobiotic transporters handle environmental compounds is likely to help increase our understanding of how these pollutants are handled and how they move through organisms and are ultimately transferred to humans. A fundamental difference between the scenario of pharmaceuticals and pollutants, is that environmental chemicals often move and amplify through multiple organisms to transfer from the environment to humans. As such the interactions of environmental chemicals with xenobiotic transporters from multiple species, at multiple levels of the food chain, are involved in the ultimate patterns of human exposure.

This study builds upon previous structural, functional, and environmental studies (Bruyere et al., 2017; Chedik et al., 2019, 2018; Epel et al., 2008; Fardel et al., 2012; Guéniche et al., 2020a, 2020b; Luckenbach and Epel, 2005; Nicklisch et al., 2017a, 2016; Smital et al., 2004; Stevenson et al., 2006) to probe potential similarities and differences in how XTs from humans and the species they consume may interact with common pollutants. It further sheds light on how chemicals that may interfere with these transporters in humans, i.e., TICs, might also act in the species that carry them. Our approach, using purified ABCB1 from wild yellowfin tuna (*Thunnus albacares*), enables direct comparison to this prior work with mammalian proteins.

4.1. Functional similarities and differences

The results revealed some important similarities and differences in the activity of *Ta*-ABCB1. Most of the tested pollutants were inhibitors of *Ta*-ABCB1, however, several interaction patterns were different for mouse and tuna (Fig. 4, Table 1). For example, at low concentrations the organochlorine pesticide TICs p,p'-DDT and its metabolite p,p'-DDD co-stimulated verapamil-induced *Ta*-ABCB1 ATPase activity, while verapamil pre-stimulated mouse ABCB1a ATPase activity was inhibited across all tested DDT and DDD concentrations (Nicklisch et al., 2016). Likewise, the flame retardant BDE-3 was able to inhibit verapamil-

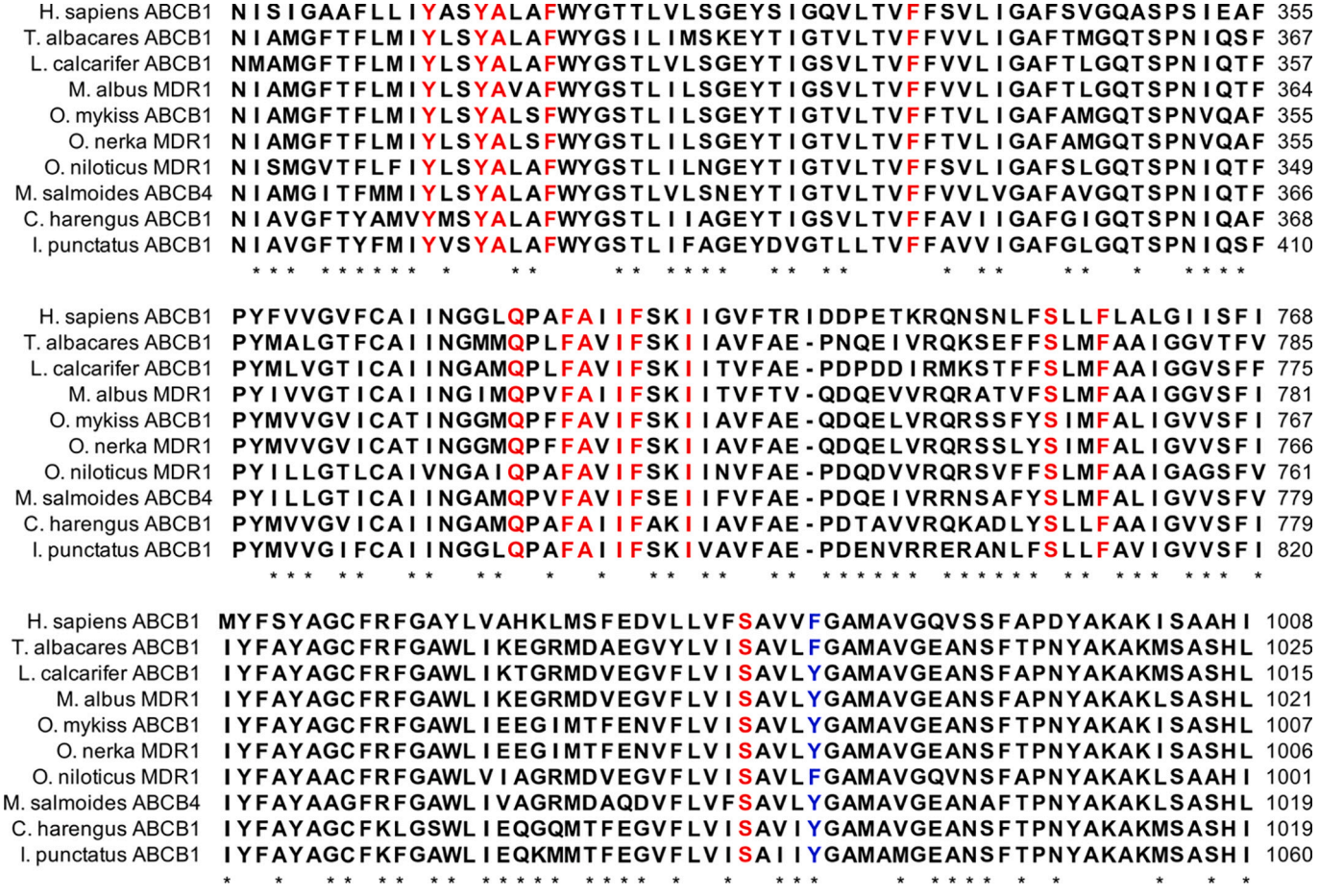

Fig. 5. Amino acid sequence alignment of BDE-100 binding residues in ABCB1 orthologs of human and commercial fish species. Highlighted are the 15 residues that interact with the bound flame retardant in the mouse ABCB1a co-crystal structure (PDB: 4XWK) (Nicklisch et al., 2016). Except for F983 (blue) in human ABCB1, all other fourteen BDE-interacting residues (red) are highly conserved across commercial fish ABCB1 proteins. Asterisks mark non-conserved residues. (For interpretation of the references to color in this figure legend, the reader is referred to the web version of this article.)

stimulated *Ta*-ABCB1 ATPase activity while pre-stimulated mouse ABCB1a showed only weak or no interaction with the compound. In contrast, the fungicide Hexachlorobenzene showed only weak interaction while the insecticide Mirex showed potent inhibition with both mouse and tuna ABCB1.

When tested against the ten previously identified TICs, *Ta*-ABCB1 showed highly similar inhibition profiles and IC_{50} values as compared to mouse, indicating a conserved mode of TIC interaction among vertebrate ABCB1. For example, the organochlorine pesticides Endrin was a strong inhibitor of ATPase activity in both tuna and mouse, with an IC_{50} value in the range of model drug inhibitor cyclosporin A. The flame retardant BDE-100, which was previously co-crystallized with mouse ABCB1a (Le et al., 2020; Nicklisch et al., 2016), showed similar interaction parameters in mouse and tuna. Furthermore, both the interaction patterns and EC_{50} values of the major DDT metabolite and TIC p,p'-DDE were similar in mouse and tuna ABCB1. Notably, the pollutant mixture representing environmental levels of nine TICs detected in yellowfin tuna caught in the Gulf of Mexico, inhibited *Ta*-ABCB1 to the same extent as mouse ABCB1a and human ABCB1 (Nicklisch et al., 2017a, 2016).

5. Conclusions and implications of TIC effects on yellowfin tuna

While the mechanisms governing accumulation of POPs in tuna and human are poorly understood, our data suggest that bio-accumulative TICs can inhibit ABCB1 function in mammals and fish and each class of TICs can interact at different ligand binding sites within ABCB1. The consequences of the inhibitory action of TICs on fish xenobiotic transporters (XTs) can be manifold. Modulating XT efflux activity can substantially increase the intracellular concentration and toxic effects of other xenobiotic substrates of these transporters, including PAHs and OCPs (Lu et al., 2014; Popovic et al., 2014; Valton et al., 2013). This is particularly important during early development where efflux transporters are highly expressed in embryos and juvenile fish to prevent xenobiotic uptake and toxicity (Brette et al., 2014; Fischer et al., 2013; Gordon et al., 2019; Incardona et al., 2014). Once in the body, TICs and other XT-evading free rider chemicals could exert sublethal toxic actions at much lower levels, specifically by impairing crucial fish sensory systems (Besson et al., 2020; Lari et al., 2020; Maryoung et al., 2015; Schlenker et al., 2019b, 2019a; Tierney et al., 2010). As structures from other xenobiotic transporters become available, the results of this study will serve as a framework to pave the way to identify additional TICs and to investigate their interactions with both ABC-type efflux transporters, including ABCB1, ABCG2, ABCC1 and ABCC2, and SLC-type uptake transporters, including Organic anion-transporting polypeptides (OATPs), Organic anion transporters (OATs), and Organic cation transporters (OCTs).

Funding information

The work of SCTN was supported by NIFA-USDA (CA-D-ETX-2526-H). The work of AH was supported by NIH grants ES027921 and 030318 and NSF 1840844.

Declaration of competing interest

The authors declare they have no actual or potential competing financial interests.

Acknowledgements

NA

Appendix A. Supplementary data

Supplementary data to this article can be found online at https://doi.org/10.1016/j.cbpc.2021.109101.

References

Ambudkar, S.V., Kimchi-Sarfaty, C., Sauna, Z.E., Gottesman, M.M., 2003. P-glycoprotein: from genomics to mechanism. Oncogene 22, 7468–7485. https://doi.org/10.1038/sj.onc.1206948.

Bai, J., Swartz, D.J., Protasevich, I.I., Brouillette, C.G., Harrell, P.M., Hildebrandt, E., Gasser, B., Mattanovich, D., Ward, A., Chang, G., Urbatsch, I.L., 2011. A gene optimization strategy that enhances production of fully functional P-glycoprotein in Pichia pastoris. PLoS One 6, e22577. https://doi.org/10.1371/journal.pone.0022577.

Besson, M., Feeney, W.E., Moniz, I., François, L., Brooker, R.M., Holzer, G., Metian, M., Roux, N., Laudet, V., Lecchini, D., 2020. Anthropogenic stressors impact fish sensory development and survival via thyroid disruption. Nat. Commun. 11 https://doi.org/10.1038/s41467-020-17450-8.

Bosch, I., Croop, J.M., 1998. P-glycoprotein structure and evolutionary homologies. Cytotechnology 27, 1–30. https://doi.org/10.1007/978-94-017-2374-9_1.

Brette, F., Machado, B., Cros, C., Incardona, J.P., Scholz, N.L., Block, B.A., 2014. Crude oil impairs cardiac excitation-contraction coupling in fish. Science (80-.). 343, 772–776. https://doi.org/10.1126/science.1242747.

Bruyere, A., Hubert, C., Le Vee, M., Chedik, L., Sayyed, K., Stieger, B., Denizot, C., Parmentier, Y., Fardel, O., 2017. Inhibition of SLC drug transporter activities by environmental bisphenols. Toxicol. in Vitro 40, 34–44. https://doi.org/10.1016/j.tiv.2016.12.009.

Callaghan, R., 2015. Providing a molecular mechanism for P-glycoprotein; why would i bother? Biochem. Soc. Trans. 43, 995–1002. https://doi.org/10.1042/BST20150131.

Campanale, J.P., Hamdoun, A., 2012. Programmed reduction of ABC transporter activity in sea urchin germline progenitors. Development 139, 783–792. https://doi.org/10.1242/dev.076752.

Chedik, L., Bruyere, A., Bacle, A., Potin, S., Le Vée, M., Fardel, O., 2018. Interactions of pesticides with membrane drug transporters: implications for toxicokinetics and toxicity. Expert Opin. Drug Metab. Toxicol. 14, 739–752. https://doi.org/10.1080/17425255.2018.1487398.

Chedik, L., Bruyere, A., Fardel, O., 2019. Interactions of organophosphorus pesticides with solute carrier (SLC) drug transporters. Xenobiotica 49, 363–374. https://doi.org/10.1080/00498254.2018.1442030.

Choy, C.A., Popp, B.N., Kaneko, J.J., Drazen, J.C., 2009. The influence of depth on mercury levels in pelagic fishes and their prey. Proc. Natl. Acad. Sci. U. S. A. 106, 13865–13869. https://doi.org/10.1073/pnas.0900711106.

Chufan, E.E., Kapoor, K., Ambudkar, S.V., 2016. Drug-protein hydrogen bonds govern the inhibition of the ATP hydrolysis of the multidrug transporter P-glycoprotein. Biochem. Pharmacol. 101, 40–53. https://doi.org/10.1016/j.bcp.2015.12.007.

Dean, M., Hamon, Y., Chimini, G., 2001. The human ATP-binding cassette (ABC) transporter superfamily. J. Lipid Res. 42, 1007–1017. https://doi.org/10.1016/s0022-2275(20)31588-1.

Epel, D., Luckenbach, T., Stevenson, C.N., MacManus-Spencer, L.A., Hamdoun, A., Smital, T., 2008. Efflux transporters: newly appreciated roles in protection against pollutants. Environ. Sci. Technol. 42, 3914–3920. https://doi.org/10.1021/es087187v.

Fardel, O., Kolasa, E., Le Vee, M., 2012. Environmental chemicals as substrates, inhibitors or inducers of drug transporters: implication for toxicokinetics, toxicity and pharmacokinetics. Expert Opin. Drug Metab. Toxicol. 8, 29–46. https://doi.org/10.1517/17425255.2012.637918.

Fischer, S., Klüver, N., Burkhardt-Medicke, K., Pietsch, M., Schmidt, A.-M.M., Wellner, P., Schirmer, K., Luckenbach, T., 2013. Abcb4 acts as multixenobiotic transporter and active barrier against chemical uptake in zebrafish (Danio rerio) embryos. BMC Biol. 11, 69. https://doi.org/10.1186/1741-7007-11-69.

Giacomini, K.M., Huang, S.M., Tweedie, D.J., Benet, L.Z., Brouwer, K.L.R., Chu, X., Dahlin, A., Evers, R., Fischer, V., Hillgren, K.M., Hoffmaster, K.A., Ishikawa, T., Keppler, D., Kim, R.B., Lee, C.A., Niemi, M., Polli, J.W., Sugiyama, Y., Swaan, P.W., Ware, J.A., Wright, S.H., Wah Yee, S., Zamek-Gliszczynski, M.J., Zhang, L., 2010. Membrane transporters in drug development. Nat. Rev. Drug Discov. 9, 215–236. https://doi.org/10.1038/nrd3028.

Gökirmak, T., Campanale, J.P., Shipp, L.E., Moy, G.W., Tao, H., Hamdoun, A., 2012. Localization and substrate selectivity of sea urchin multidrug (MDR) efflux transporters. J. Biol. Chem. 287, 43876–43883. https://doi.org/10.1074/jbc.M112.424879.

Gökirmak, T., Shipp, L.E., Campanale, J.P., Nicklisch, S.C.T., Hamdoun, A., 2014. Transport in technicolor: mapping ATP-binding cassette transporters in sea urchin embryos. Mol. Reprod. Dev. 81, 778–793. https://doi.org/10.1002/mrd.22357.

Gokirmak, T., Campanale, J.P., Reitzel, A.M., Shipp, L.E., Moy, G.W., Hamdoun, A., 2016. Functional diversification of sea urchin ABCC1 (MRP1) by alternative splicing. Am. J. Physiol. Cell Physiol. 1, ajpcell 00029, 2016. https://doi.org/10.1152/ajpcell.00029.2016.

Gordon, W.E., Espinoza, J.A., Leerberg, D.M., Yelon, D., Hamdoun, A., 2019. Xenobiotic transporter activity in zebrafish embryo ionocytes. Aquat. Toxicol. 212, 88–97. https://doi.org/10.1016/j.aquatox.2019.04.013.

Guéniche, N., Bruyere, A., Le Vée, M., Fardel, O., 2020a. Implication of human drug transporters to toxicokinetics and toxicity of pesticides. Pest Manag. Sci. 76, 18–25. https://doi.org/10.1002/ps.5577.

Guéniche, N., Bruyere, A., Ringeval, M., Jouan, E., Huguet, A., Le Hégarat, L., Fardel, O., 2020b. Differential interactions of carbamate pesticides with drug transporters. Xenobiotica 50, 1380–1392. https://doi.org/10.1080/00498254.2020.1771473.

Gutmann, D.A.P., Ward, A., Urbatsch, I.L., Chang, G., van Veen, H.W., 2010. Understanding polyspecificity of multidrug ABC transporters: closing in on the gaps in ABCB1. Trends Biochem. Sci. 35, 36–42. https://doi.org/10.1016/j.tibs.2009.07.009.

Holme, J.A., Brinchmann, B.C., Refsnes, M., Låg, M., Øvrevik, J., 2019. Potential role of polycyclic aromatic hydrocarbons as mediators of cardiovascular effects from combustion particles. Environ. Heal. A Glob. Access Sci. Source. https://doi.org/10.1186/s12940-019-0514-2.

Incardona, J.P., Collier, T.K., Scholz, N.L., 2004. Defects in cardiac function precede morphological abnormalities in fish embryos exposed to polycyclic aromatic hydrocarbons. Toxicol. Appl. Pharmacol. 196, 191–205. https://doi.org/10.1016/j.taap.2003.11.026.

Incardona, J.P., Carls, M.G., Teraoka, H., Sloan, C.A., Collier, T.K., Scholz, N.L., 2005. Aryl hydrocarbon receptor-independent toxicity of weathered crude oil during fish development. Environ. Health Perspect. 113, 1755–1762. https://doi.org/10.1289/ehp.8230.

Incardona, J.P., Carls, M.G., Day, H.L., Sloan, C.A., Bolton, J.L., Collier, T.K., Schoiz, N. L., 2009. Cardiac arrhythmia is the primary response of embryonic pacific herring (Clupea pallasi) exposed to crude oil during weathering. Environ. Sci. Technol. 43, 201–207. https://doi.org/10.1021/es802270t.

Incardona, J.P., Swarts, T.L., Edmunds, R.C., Linbo, T.L., Aquilina-Beck, A., Sloan, C.A., Gardner, L.D., Block, B.A., Scholz, N.L., 2013. Exxon Valdez to Deepwater horizon: comparable toxicity of both crude oils to fish early life stages. Aquat. Toxicol. 142–143, 303–316. https://doi.org/10.1016/j.aquatox.2013.08.011.

Incardona, J.P., Gardner, L.D., Linbo, T.L., Brown, T.L., Esbaugh, A.J., Mager, E.M., Stieglitz, J.D., French, B.L., Labenia, J.S., Laetz, C. a, Tagal, M., Sloan, C. a, Elizur, A., Benetti, D.D., Grosell, M., Block, B. a, Scholz, N.L., 2014. PNAS plus: from the cover: Deepwater horizon crude oil impacts the developing hearts of large predatory pelagic fish. Proc. Natl. Acad. Sci. 111, E1510–E1518. https://doi.org/10.1073/pnas.1320950111.

Laemmli, U.K., 1970. Cleavage of structural proteins during the assembly of the head of bacteriophage T4. Nature 227, 680–685. https://doi.org/10.1038/227680a0.

Lari, E., Burket, S.R., Steinkey, D., Brooks, B.W., Pyle, G.G., 2020. Interaction of the olfactory system of rainbow trout (Oncorhynchus mykiss) with Diltiazem. Environ. Toxicol. Chem. 00, 1–7. https://doi.org/10.1002/etc.4854.

Le, C.A., Harvey, D.S., Aller, S.G., 2020. Structural definition of polyspecific compensatory ligand recognition by P-glycoprotein. IUCrJ 7, 663–672. https://doi.org/10.1107/S2052252520005709.

Litman, T., Zeuthen, T., Skovsgaard, T., Stein, W.D., 1997. Competitive, non-competitive and cooperative interactions between substrates of P-glycoproteins as measured by ATPase activity. Biochim. Biophys. Acta Mol. basis Dis. 1361, 169–176. https://doi.org/10.1016/S0925-4439(97)00027-6.

Litman, T., Brangi, M., Hudson, E., Fetsch, P., Abati, A., Ross, D.D., Miyake, K., Resau, J. H., Bates, S.E., 2000. The multidrug-resistant phenotype associated with overexpression of the new ABC half-transporter, MXR (ABCG2). J. Cell Sci. 113, 2011–2021.

Liu, S., Li, Q., Liu, Z., 2013. Genome-wide identification, characterization and phylogenetic analysis of 50 catfish ATP-binding cassette (ABC) transporter genes. PLoS One 8, e63895. https://doi.org/10.1371/journal.pone.0063895.

Lu, X., Long, Y., Lin, L., Sun, R., Zhong, S., Cui, Z., 2014. Characterization of zebrafish Abcc4 as an efflux transporter of organochlorine pesticides. PLoS One 9, e111664. https://doi.org/10.1371/journal.pone.0111664.

Luckenbach, T., Epel, D., 2005. Nitromusk and polycyclic musk compounds as long-term inhibitors of cellular xenobiotic defense systems mediated by multidrug transporters. Environ. Health Perspect. 113, 17–24. https://doi.org/10.1289/ehp.7301.

Luckenbach, T., Fischer, S., Sturm, A., 2014. Current advances on ABC drug transporters in fish. Comp. Biochem. Physiol. Part - C Toxicol. Pharmacol. 165, 28–52. https://doi.org/10.1016/j.cbpc.2014.05.002.

Marris, C.R., Kompella, S.N., Miller, M.R., Incardona, J.P., Brette, F., Hancox, J.C., Sørhus, E., Shiels, H.A., 2020. Polyaromatic hydrocarbons in pollution: a heart-breaking matter. J. Physiol. 598, 227–247. https://doi.org/10.1113/JP278885.

Maryoung, L.A., Blunt, B., Tierney, K.B., Schlenk, D., 2015. Sublethal toxicity of chlorpyrifos to salmonid olfaction after hypersaline acclimation. Aquat. Toxicol. 161, 94–101. https://doi.org/10.1016/j.aquatox.2015.01.026.

Morrissey, K.M., Wen, C.C., Johns, S.J., Zhang, L., Huang, S.M., Giacomini, K.M., 2012. The UCSF-FDA transportal: a public drug transporter database. Clin. Pharmacol. Ther. 92, 545–546. https://doi.org/10.1038/clpt.2012.44.

Nicklisch, S.C.T., Hamdoun, A., 2020. Disruption of small molecule transporter systems by transporter-interfering chemicals (TICs). FEBS Lett. 594, 4158–4185. https://doi.org/10.1002/1873-3468.14005.

Nicklisch, S.C.T., Rees, S.D., McGrath, A.P., Gökirmak, T., Bonito, L.T., Vermeer, L.M., Cregger, C., Loewen, G., Sandin, S., Chang, G., Hamdoun, A., 2016. Global marine pollutants inhibit P-glycoprotein: environmental levels, inhibitory effects, and cocrystal structure. Sci. Adv. 2 https://doi.org/10.1126/sciadv.1600001.

Nicklisch, S.C.T., Bonito, L.T., Sandin, S., Hamdoun, A., 2017a. Geographic differences in persistent organic pollutant levels of yellowfin tuna. Environ. Health Perspect. 125, 1–13. https://doi.org/10.1289/EHP518.

Nicklisch, S.C.T., Bonito, L.T., Sandin, S., Hamdoun, A., 2017b. Mercury levels of yellowfin tuna (Thunnus albacares) are associated with capture location. Environ. Pollut. 229, 87–93. https://doi.org/10.1016/j.envpol.2017.05.070.

Orlowski, S., Mir, L.M., Belehradek, J., Garrigos, M., 1996. Effects of steroids and verapamil on P-glycoprotein ATPase activity: progesterone, desoxycorticosterone, corticosterone and verapamil are mutually non-exclusive modulators. Biochem. J. 317, 515–522. https://doi.org/10.1042/bj3170515.

Palmeira, A., Sousa, E.H., Vasconcelos, M., Pinto, M., 2012. Three decades of P-gp inhibitors: skimming through several generations and scaffolds. Curr. Med. Chem. 19, 1946–2025. https://doi.org/10.2174/092986712800167392.

Pecoraro, C., Zudaire, I., Bodin, N., Murua, H., Taconet, P., Díaz-Jaimes, P., Cariani, A., Tinti, F., Chassot, E., 2017. Putting all the pieces together: integrating current knowledge of the biology, ecology, fisheries status, stock structure and management of yellowfin tuna (Thunnus albacares). Rev. Fish Biol. Fish. 27, 811–841. https://doi.org/10.1007/s11160-016-9460-z.

Pecoraro, C., Babbucci, M., Franch, R., Rico, C., Papetti, C., Chassot, E., Bodin, N., Cariani, A., Bargelloni, L., Tinti, F., 2018. The population genomics of yellowfin tuna (Thunnus albacares) at global geographic scale challenges current stock delineation. Sci. Rep. 8, 1–10. https://doi.org/10.1038/s41598-018-32331-3.

Popovic, M., Zaja, R., Fent, K., Smital, T., 2014. Interaction of environmental contaminants with zebrafish organic anion transporting polypeptide, Oatp1d1 (Slco1d1). Toxicol. Appl. Pharmacol. 280, 149–158. https://doi.org/10.1016/j.taap.2014.07.015.

Pulster, E.L., Gracia, A., Armenteros, M., Toro-Farmer, G., Snyder, S.M., Carr, B.E., Schwaab, M.R., Nicholson, T.J., Mrowicki, J., Murawski, S.A., 2020. A first comprehensive baseline of hydrocarbon pollution in Gulf of Mexico fishes. Sci. Rep. 10, 1–14. https://doi.org/10.1038/s41598-020-62944-6.

Robey, R.W., Robinson, A.N., Ali-rahmani, F., Huff, L.M., Lusvarghi, S., Vahedi, S., Hotz, J., Warner, A.C., Butcher, D., Matta, J., Elijah, F., Lee, T.D., Roth, J.S., Lee, O. W., Shen, M., Tanner, K., Hall, M.D., Ambudkar, S.V., Gottesman, M.M., 2021. Characterization and Tissue Localization of Zebrafish Homologs of the Human ABCB1 Multidrug Transporter. bioRxiv. https://doi.org/10.1101/2021.02.18.431829.

Schlenker, L.S., Welch, M.J., Mager, E.M., Stieglitz, J.D., Benetti, D.D., Munday, P.L., Grosell, M., 2019a. Exposure to crude oil from the Deepwater horizon oil spill impairs oil avoidance behavior without affecting olfactory physiology in juvenile Mahi-Mahi (Coryphaena hippurus). Environ. Sci. Technol. 53, 14001–14009. https://doi.org/10.1021/acs.est.9b05240.

Schlenker, L.S., Welch, M.J., Meredith, T.L., Mager, E.M., Lari, E., Babcock, E.A., Pyle, G. G., Munday, P.L., Grosell, M., 2019b. Damsels in distress: oil exposure modifies behavior and olfaction in bicolor damselfish (Stegastes partitus). Environ. Sci. Technol. 53, 10993–11001. https://doi.org/10.1021/acs.est.9b03915.

Shapiro, A.B., Ling, V., 1997. Positively cooperative sites for drug transport by P-glycoprotein with distinct drug specificities. Eur. J. Biochem. 250, 130–137. https://doi.org/10.1111/j.1432-1033.1997.00130.x.

Shapiro, A.B., Fox, K., Lam, P., Ling, V., 1999. Stimulation of P-glycoprotein-mediated drug transport by prazosin and progesterone: evidence for a third drug-binding site. Eur. J. Biochem. 259, 841–850. https://doi.org/10.1046/j.1432-1327.1999.00098.x.

Shipp, L.E., Hill, R.Z., Moy, G.W., Gökırmak, T., Hamdoun, A., 2015. ABCC5 is required for cAMP-mediated hindgut invagination in sea urchin embryos. Development 142, 3537–3548. https://doi.org/10.1242/dev.126144.

Smital, T., Luckenbach, T., Sauerborn, R., Hamdoun, A.M., Vega, R.L., Epel, D., 2004. Emerging contaminants - pesticides, PPCPs, microbial degradation products and natural substances as inhibitors of multixenobiotic defense in aquatic organisms. Mutat. Res. Fundam. Mol. Mech. Mutagen. 552, 101–117. https://doi.org/10.1016/j.mrfmmm.2004.06.006.

Sreeramulu, K., Liu, R., Sharom, F.J., 2007. Interaction of insecticides with mammalian P-glycoprotein and their effect on its transport function. Biochim. Biophys. Acta Biomembr. 1768, 1750–1757. https://doi.org/10.1016/j.bbamem.2007.04.001.

Stevenson, C.N., Macmanus-Spencer, L.A., Luckenbach, T., Luthy, R.G., Epel, D., 2006. New perspectives on perfluorochemical ecotoxicology: inhibition and induction of an efflux transporter in the marine mussel, Mytilus californianus. Environ. Sci. Technol. 40, 5580–5585. https://doi.org/10.1021/es0602593.

Swartz, D.J., Weber, J., Urbatsch, I.L., 2013. P-glycoprotein is fully active after multiple tryptophan substitutions. Biochim. Biophys. Acta Biomembr. 1828, 1159–1168. https://doi.org/10.1016/j.bbamem.2012.12.005.

Tierney, K.B., Baldwin, D.H., Hara, T.J., Ross, P.S., Scholz, N.L., Kennedy, C.J., 2010. Olfactory toxicity in fishes. Aquat. Toxicol. 96, 2–26. https://doi.org/10.1016/j.aquatox.2009.09.019.

Valton, E., Amblard, C., Wawrzyniak, I., Penault-Llorca, F., Bamdad, M., 2013. P-gp expression in brown trout erythrocytes: evidence of a detoxification mechanism in fish erythrocytes. Sci. Rep. 3, 1–5. https://doi.org/10.1038/srep03422.

van Den Elsen, J.M., Kuntz, D.A., Hoedemaeker, F.J., Rose, D.R., 1999. Antibody C219 recognizes an alpha-helical epitope on P-glycoprotein. Proc. Natl. Acad. Sci. U. S. A. 96, 13679–13684. https://doi.org/10.1073/pnas.96.24.13679.

Xie, J., Bian, Z., Lin, T., Tao, L., Wu, Q., Chu, M., 2020. Global occurrence, bioaccumulation factors and toxic effects of polychlorinated biphenyls in tuna: a review. Emerg. Contam. 6, 388–395. https://doi.org/10.1016/j.emcon.2020.11.003.